Trapping gap solitons in a resonant photonic crystal of finite length

Wanneng Xiao*
Faculty of Physics and Optoelectronic Engineering, Guangdong University of Technology, Guangzhou 510090, China
(Received 23 September 2006; revised manuscript received 10 April 2007; published 26 June 2007)

The finite-length effect of a resonant nonlinear photonic crystal on the propagation dynamics of gap solitons is theoretically studied. This effect results in a dissipation and deceleration of the moving gap solitons such that the propagation dynamics is essentially different from that on an infinite domain. Due to this effect, two slow counterpropagating solitons can collide into a nonmoving breatherlike bound state, even under many realistic excitation circumstances.

DOI: 10.1103/PhysRevE.75.066610 PACS number(s): 42.81.Dp, 42.70.Qs, 42.65.Tg, 02.30.Jr

I. INTRODUCTION

The dynamics of light propagation in nonlinear photonic crystals (PC) has been of great research interest over the past decade [1]. The refractive index of a PC is periodically modulated, which creates a linear forbidden spectral band known as photonic band gap (PBG) [1]. Further embedding thin layers of nonlinear medium periodically [2–4] in a linear PC results in a nonlinear one, which, however, permits an intense pulse to propagate through the linear PBG in the form of spatially localized bright region called the gap soliton (GS) [5–8]. A GS originates from the intricate balance between linear dispersion, Bragg reflection, and self-focusing nonlinearity and consists of, unlike solitons in a nonlinear uniform medium, two components of the forward- and backward-propagating waves traveling at the same group velocity [2,3]. Many experimental observations of GSs have been reported in different types of nonlinear PC structures [9–12]. Further, the research interest evolves toward developing various ways to trap the GSs for obtaining stopped light. Several theoretical works [13–15] predicted that this goal can be achieved by using a coherent or incoherent pump to create a steady-state local defect within the PC structures for trapping the moving GSs.

However, to our best knowledge, in current theoretical works the structural length of a nonlinear PC is just assumed to be infinite so that the corresponding mathematic model can be simplified to an integrable system and be resolved analytically [8,16,17]. Although this assumption often makes no obvious influence to the results when the medium is long enough and the incident light is intense, it is in principle untrue since a practical structure always has the limited length. Qualitatively, due to the finite length itself as well as the induced boundary conditions, either the linear PBG or nonlinear GS actually becomes different from its counterpart obtained on an infinite domain. Specifically, the former is no longer 100% linearly reflective; the latter is truncated at the two boundaries and hence the inner balance of it is destroyed. In this paper, we investigate this effect on the propagation dynamics of GSs and find it substantially changes the behaviors of those GSs with their initial velocity slow enough. Based on this finding, a feasible way to trap slow GSs in a stable bound state is demonstrated under many realistic excitation conditions.

*zhongshuq@tom.com

II. THEORETICAL MODEL AND ANALYSIS

The model we study here is a resonantly absorbing Bragg-periodic reflector (RABR) [2,3,18], which is formed by Bragg-periodically embedding thin layers of resonantly absorbing two-level systems (atoms, ions, or excitons) into a one-dimensional nonabsorbing linear uniform medium and hence has the resonant nonlinearity. In contrast to the cubic nonlinear GSs excited in Kerr nonlinear PCs [9,14,19–21] (where very intense light pulses of 10 GW/cm^2 or greater were required), the resonant GSs in a RABR have been predicted to form by a principally different mechanism at much lower input intensities (10 MW/cm^2 or less) [3,15,22,23], which is significant for practical applications. This model closely corresponds to a real structure of Bragg-periodically arranged quantum wells with resonant excitons in a semiconductor, which has been successfully fabricated and whose linear and nonlinear properties have been studied experimentally [4,18]. The theory used here for this model is based on the coupled-mode two-wave Maxwell-Bloch (TWMB) equations in the slowly varying envelope approximation of the forward and backward propagating electric fields $E^{\pm}(x,t)$, which can be expressed in terms of the real valued functions as [2,13,15]

$$\Omega_t^{\pm}(x,t) \pm \Omega_x^{\pm}(x,t) = P(x,t), \tag{1a}$$

$$P_t(x,t) = n(x,t)[\Omega^+(x,t) + \Omega^-(x,t)], \tag{1b}$$

$$n_t(x,t) = -\mathrm{Re}\{P^*(x,t)[\Omega^+(x,t) + \Omega^-(x,t)]\}, \tag{1c}$$

where $\Omega^{\pm}(x,t) = (2\tau_c\mu/\hbar)E^{\pm}(x,t)$; $E^{\pm}(x,t)$ are the smooth field-amplitude envelopes of the forward and backward Bloch waves; $\tau_c = (8\pi\epsilon T_1/3c\rho\lambda^2)^{1/2}$ is the cooperative time, characterizing the mean photon lifetime in the medium preceding resonant absorption; ϵ is the dielectric constant of the medium; T_1 is the longitudinal relaxation time of the Bloch vector; ρ is the density of two-level systems; λ is the wavelength of the propagating light field (note in this model, the light pulse is just assumed as a quasimonochromatic scalar field, and its frequency is exactly resonant to the two-level systems); μ is the matrix element of the dipole transition moment; $P(x,t)$ and $n(x,t)$ are the polarization and density of inverse population, respectively; c is the speed of light in vacuum; $t = t'/\tau_c$ and $x = x'/c\tau_c$ are, respectively, the dimensionless time and space variables, where t' and x' represent the real physical time and spatial coordinates along the nor-

 ©2007 The American Physical Society

mal to the resonance planes in the structure, respectively; and the subscripts x and t imply partial derivatives. Considering the extremely compact notation of the model, without losing generality a theoretical treatment can be just in scaled units of the cooperative time τ_c, i.e., $\tau_c=1$. Experimentally, its value can be readily set for specific applications by selecting the suitable material parameters such as density and oscillator strength since they are contained in τ_c. For instance, $\tau_c \approx 0.6$ ps in a RABR consisting of GaAs quantum wells with two-dimensional excitons when the exciton density $\rho=2\times10^{19}$ m^{-3} and the wavelength $\lambda=806$ nm.

Further, substituting solutions of the Bloch equation $P=-\sin\theta$ and $n=-\cos\theta$ into Eq. (1) gives rise to the exact 1D sine-Gordon equation (SGE) [2]

$$\theta_{xx}-\theta_{tt}=\sin\theta. \tag{2}$$

The quantity θ denotes the Bloch phase angle and is closely related to the propagating fields by the equation $\theta(x,t)=\int_{-\infty}^{t}\Omega(x,t')dt'$, where $\Omega=\Omega^{+}+\Omega^{-}$. If the length of a RABR is taken as infinite, i.e., the boundary constraint can be described as $\theta\to0$ and $d\theta/dx\to0$ as $x\to\pm\infty$, then the dynamics equation of SGE (2) becomes a completely integrable system and can be analytically resolved. The solutions include a complete set of localized traveling waves: solitons [17]. The two simplest ones (one-soliton) of them are the kink and antikink. Other higher-order ones are called N solitons and can be obtained either by the Bäcklund transformation [8] or by the direct method [17]. However, for a practical RABR of finite length, the dynamics system includes not only the universal equation (2) but also the practical boundary conditions of free input or output of energies so that it becomes nonconservative (hence nonintegrable) and, at least in principle, can no longer be resolved analytically.

To clarify the difference between these two situations of infinite and finite, we first qualitatively discuss the finite-length effect in a way of energetic analysis combined with physical intuition. Let us begin with the general localized solutions to SGE (2) on an infinite domain, among which we are interested in these four ones closely related to this work: kink θ_{+}, antikink θ_{-}, kink-antikink two-soliton (K-$\bar{K}$) $\theta^{K\bar{K}}$, and breather θ^{br}. They can be explicitly expressed as [16,17]

$$\theta_{\pm}(x,t)=4\tan^{-1}\left[\exp\left(\pm\frac{x-ut-x_0}{\sqrt{1-u^2}}\right)\right], \tag{3a}$$

$$\theta^{K\bar{K}}(x,t)=4\tan^{-1}\left(\frac{\sinh[u(t-t_0)/\sqrt{1-u^2}]}{u\cosh[(x-x_0)/\sqrt{1-u^2}]}\right), \tag{3b}$$

$$\theta^{\mathrm{br}}(x,t)=4\tan^{-1}\left(\frac{\tan\nu\sin[(\cos\nu)(t-t_0)]}{\cosh[(\sin\nu)(x-x_0)]}\right). \tag{3c}$$

The parameters u and x_0 in $\theta_{\pm}(x,t)$ denote, respectively, the constant velocity and initial center of the one-soliton. This velocity u can take any value between -1 and $+1$, i.e., $-1<u<1$. The parameter u in the second expression also has the meaning of velocity but obviously cannot take 0, x_0 here denotes the initial position of the mass center of a K-$\bar{K}$. The parameter ν in the third determines the breather shape and size and has $\nu\neq\pi$. Note that $\theta^{K\bar{K}}$ can be readily obtained from the two single solitons $\theta_{\pm}$ by using the Bäcklund transformation, but the breather θ^{br} cannot from them. In addition, the Hamiltonian for the perfect SGE of Eq. (2) on an infinite line is

$$\boldsymbol{H}\equiv\int_{-\infty}^{+\infty}\left(\frac{1}{2}\theta_t^2+\frac{1}{2}\theta_x^2+1-\cos\theta\right)dx. \tag{4}$$

Substituting Eq. (3) into (4), we obtain the total energy for these four solitons $E_{\pm}=8/(1-u^2)^{1/2}\geq8$, $E^{K\bar{K}}=16/(1-u^2)^{1/2}>16>16\sin\nu=E^{\mathrm{br}}$. This means that, in a conservative system a pair of kink and antikink always has more energy than a breather and can never combine into it, which is exactly in accordance with the result from the Bäcklund transformation. In addition, on an infinite domain a GS is exactly balanced and always preserves its energy and velocity during the propagation or collision with others. Thus, a pair of kink and antikink can never give rise to a breather by collision with each other, i.e., trapping of them in this way is impossible on an infinite domain.

However, in a real physical model, this conclusion probably becomes invalid due to the finite-length effect. First, the kink or antikink is actually truncated at the two boundaries so that its energy becomes

$$E_{\pm}^{\mathrm{real}}=\frac{16}{\sqrt{1-u^2}}\left(2-\frac{1}{1+\exp\left(\pm2\dfrac{x_1-ut-x_0}{\sqrt{1-u^2}}\right)}-\frac{1}{1+\exp\left(\pm2\dfrac{x_2-ut-x_0}{\sqrt{1-u^2}}\right)}\right). \tag{5}$$

Obviously, $E_{\pm}^{\mathrm{real}}$ is the function of u, x_1, and x_2, and can possibly be less than 8. Further, since such a truncated soliton is no longer an exact equilibrium state, during its propagation it necessarily tries to gradually modify its form toward a perfect kink or antikink of the infinite domain. This modification can only be fulfilled by ceaselessly emitting the fast linear waves out of the structure (remember that the PBG of a finite structure is no more fully forbidden to linear light field), and hence also results in energy leakages of a GS. On the other hand, the velocity of the GS is also gradually decelerated since it is proportional to the energy. Thus, a truncated GS of the practical structures has the chance to arrive at a state of $u=0$, which means the GS is trapped within the structure. Nevertheless, such a singly trapped GS has proved unstable and will eventually be nonlinearly reflected or transmitted [13]. However, if we at the same time excite a similar one from the opposite direction to make them collide with each other, they may combine into a stable bound state, which actually corresponds to a breather created by a pair of truncated kink and antikink and, according to the analysis above, obviously can also satisfy the energy requirement.

To check whether this is the truth, let us directly solve Eq. (1) numerically under the set of initial and boundary conditions

$$\Omega^+(x=0,t)=\Omega^+(t), \tag{6a}$$

$$\Omega^-(x=l,t)=\Omega^-(t), \tag{6b}$$

$$\Omega^{\pm}(x,t=0)=0, \tag{6c}$$

$$P(x,t=0)=0, \tag{6d}$$

$$n(x,t=0)=-1, \tag{6e}$$

which corresponds to a quite realistic experimental configuration. The character of the structure depends only on the parameter of length l and different excitation conditions can be obtained by varying the amplitude and shape of the input field $\Omega^{\pm}(t)$.

III. NUMERICAL RESULTS AND DISCUSSIONS

We solve this nonintegrable system of Eqs. (1) and (6) by the finite-difference time-domain method for various structural lengths l (finite) and find that, the anticipated breatherlike bound state always really can be achieved by setting a suitable incident intensity according to the specific l. The fact that the occurrence of the bound state is independent of length is understandable because the finite-length effect, which is responsible for the bound state, always exists if only the structure is not infinite. Thus, to investigate the common property of the propagation and collision dynamics in a finite RABR structure, we only need to focus on the intensity and profile of the incident pulses. Generally, our results show: for any a given length, there always exists a threshold regime of the incident intensity, within which two counterpropagating GSs can coalesce into the breatherlike bound state, while below or above which they are just linearly reflected out or unaffectedly pass through each other just like what occurs on an infinite domain. This means that the finite-length effect makes apparent importance mainly to those GSs of moderate energy or velocity, but is hardly perceptible under the circumstance of intense or weak excitation. That is why it has not been realized in current theoretical works.

Without losing generality, all results below are for a typical length of $l=40$ (in units of $c\tau_c$), which corresponds to a practical InGaAs multiquantum wells sample with the physical length of 7.2 mm and consisting of about 65 000 layers. We first assume that it is excited by a pair of similar smooth sech pulses from the two opposite boundaries. The reason why the sech-like incident field is selected is that the area of a left- or right-moving sech pulse exactly corresponds to a kink or antikink solution of the SGE, respectively. Thus, the amplitude of incident electric field can be expressed as

$$\Omega_0^+(t)=\Omega_l^-(t)=\Omega_0\,\mathrm{sech}[(t-t_p)/\tau_0), \tag{7}$$

where Ω_0, t_p, and τ_0 are the excitation parameters of peak value, time delay, and duration of the incident pulses, respectively. Here we set $t_p=5$ to ensure the pulses enter from far away, and simply let the pulse duration $\tau_0\equiv 0.5$ (in units of τ_c), corresponding to a practical femtosecond laser pulse. Then, the pulse area θ, determining the incident intensity, can be arbitrarily adjusted only by varying the peak value Ω_0.

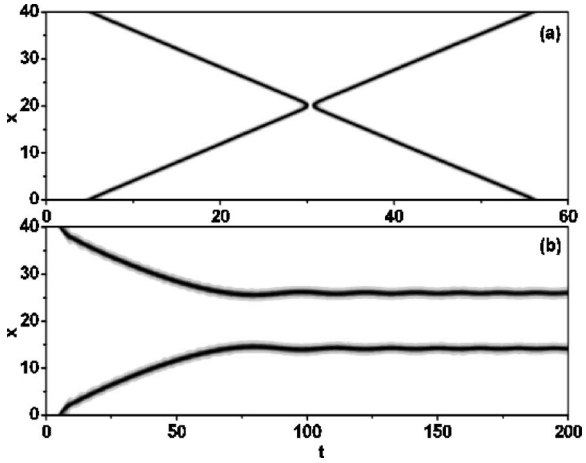

FIG. 1. Contour plot for the spatiotemporal evolution of inversion $n(x,t)$ within a RABR excited by two counterinfused sech pulses with equivalent peak value of (a) $\Omega_0=4.30$, (b) $\Omega_0=3.58$. The black corresponds to $n=1$, i.e., population inversion, and the white to $n=-1$, two-level systems in ground state.

Typical outcomes under sech-like excitations of different intensities are illustrated in Figs. 1 and 2. When the incident intensity is too high [Fig. 1(a) with $\Omega_0=4.3$], there is no obvious evidence of deceleration in the GSs. Further increasing of the incident intensity brings no substantial difference, indicating that the excitation of $\Omega_0\geq 4.3$ belongs to a strong nonlinear regime for the length of $l=40$ and is almost not subject to the finite-length effect. In the other limit, when the incident intensity is lowered to $\Omega_0=3.58$ [Fig. 1(b)], this effect strongly emerges by causing so striking a deceleration in the GSs that they have already stopped before collision. Below this value of excitation, the dynamics system falls into the linear regime, i.e., the incident light is just Bragg reflected and no GS is excited. Thus, $3.58<\Omega_0<4.3$ is ac-

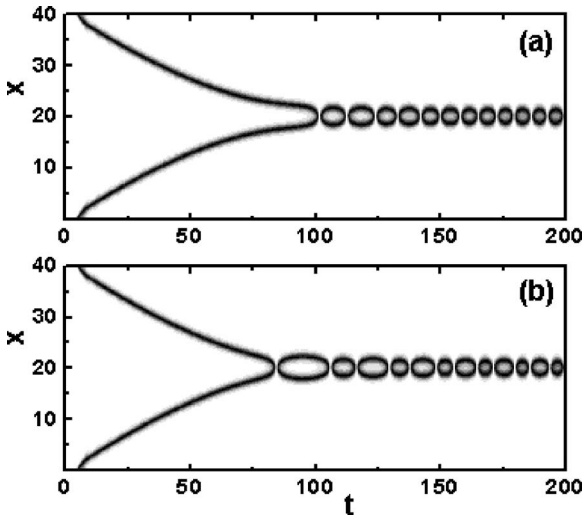

FIG. 2. Evolution of $n(x,t)$ under excitation by a sech pulse pair of the peak value $\Omega_0=3.59$ but with the profile being (a) smooth, (b) perturbed by white noises of ratio 15% to the original.

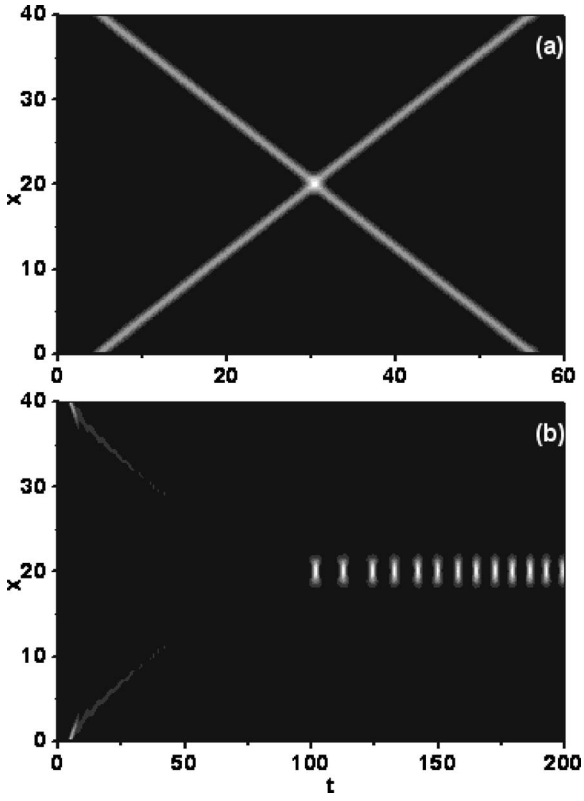

FIG. 3. Evolution of the field intensity under the same excitation condition as that for (a) Fig. 1(a), (b) Fig. 2(a). The brightness is proportional to $\ln[1+\Omega^2(x,t)]$.

tually the critical regime for the length of $l=40$ to display the finite-length effect. Certainly, other lengths also have their own critical regimes, whose value and broadness both grow along with the increase of structural length. A typical result of GS interaction within this regime is shown in Fig. 2(a) with $\Omega_0=3.59$. The two decelerated GSs just coalesce into a quiescent bound state, whose energy periodically oscillates between localized atomic excitation and coherent light. The stability of it is displayed in Fig. 2(b), where a quite large white noise (15% of the origin signal) is added up to the incident field by multiplying the term of $1+0.3[\text{rand}(t)-0.5]$ ["rand(t)" stands for the random function and it arbitrarily creates values from 0 to 1] to the originally smooth envelope. The noises obviously do not qualitatively damage the occurrence and existence of the bound state.

For comparison, the evolution of the other important quantity (the light field) is also demonstrated in Fig. 3, where the light intensity rather than the field amplitude is adopted since the former is more meaningful for detecting. In addition, note that the intensity in Fig. 3 is plotted on the natural logarithmic scale, i.e., the brightness is proportional to the quantity of $\ln[1+\Omega^2(x,t)]$. This treatment is in order to distinguish those very small intensities, since the light intensity is found to actually vary within a very wide range during its propagation. The excitation conditions for Figs. 3(a) and 3(b) correspond, respectively, to those of Figs. 1(a) and 2(a). In both cases, the light field and population inversion evolve almost in the similar way. The total energy of a GS is actually divided into two parts—the population inversion and the

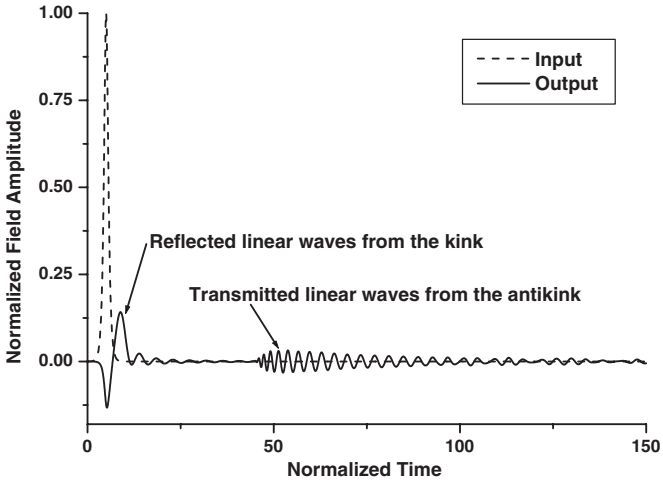

FIG. 4. Amplitude $\Omega(t)$ of the input (dashed line) and output (solid line) optical field at the left end of the RABR structure under the excitation condition of Fig. 2(a).

light field, both propagating together in the same velocity at any time. Further, note that the inversion can be saturated and hence has a maximum value, while the light field can carry arbitrary energy. Thus, if the input energy (always first satisfies the requirement of population inversion) is not large enough, the light field may disappear [see the duration after the linear radiations and before the coalescence in Fig. 3(b)]. The evolutions of light field for other conditions (not provided) are also exactly corresponds to those of inversion, so the following results are shown only by the population inversion.

According to our analysis, it is the linear radiations released from a GS that directly result in the deceleration and coalescence. However, they can hardly be observed just from the plots of $n(x,t)$ or $\Omega^2(x,t)$ since they are much weaker than a GS. Thus, to clearly witness the existence of them the best way is to monitor the energy fluxes in and out of the structure from the two boundaries. Note that the dynamical fluxes through both boundaries actually are exactly the same since the excitation is completely symmetric. Hence, we need provide only one of them. This is shown in Fig. 4, demonstrating the field amplitude fluxes in (dashed) and out (solid) of one endpoint under the excitation condition of Fig. 2(a). The corresponding energy fluxes can be obtained by squaring this field amplitude. Clearly, the outward flux consists of two chains of linear waves, emerging shortly and long after the input field enters into the structure, respectively. In fact, for the left boundary they are, respectively, backward linear radiations of the right-moving kink and forward ones of the left-moving antikink, and vice versa for the right boundary. Note again such separating of linear radiations from a GS will never occur on an infinite domain, since where a GS is exactly balanced and strictly self-preserving.

Further, to validate our numerical results we also provide the analytic counterparts in Fig. 5 for comparison. They are obtained by directly substituting the analytic solutions of Eqs. (3b) and (3c), respectively, into the expression $n(x,t)=-\cos\theta(x,t)$, one solution of the Bloch equation. Comparing Figs. 1(a) and 2(a), respectively, with Figs. 5(a) and 5(b), we

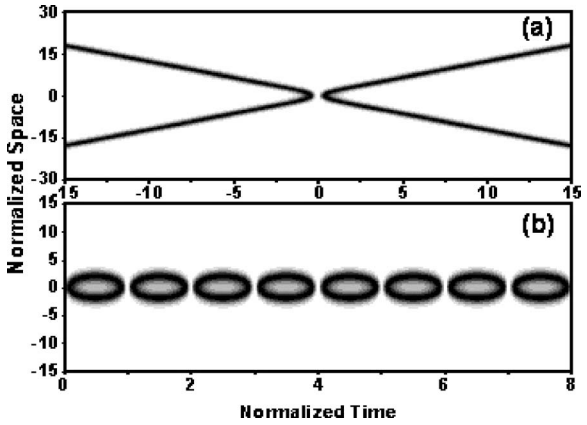

FIG. 5. Evolution of analytic $n(x,t)$ derived from the two-soliton solution of (a) K-$\bar{K}$ described by Eq. (3b) with $u=0.5$ and the scaled time t and space x to $(1/u^2-1)^{1/2}$ and $(1-1/u^2)^{1/2}$, respectively. (b) Breather by Eq. (3c) with $\nu=1.3$ and t and x scaled to $\cos \nu/\pi$ and $\sin \nu$, respectively. Other parameters are set as $x_0=t_0=0$ for both.

readily find the common properties in both cases, which confirms our former predictions especially that the final bound state formed by two decelerated GSs is breatherlike.

Finally, we investigate how this effect works on the results for more critical and realistic conditions and find that the finite-length-induced stable bound state can also occur under at least three other kinds of excitations by: nonsymmetric sech pulses [Fig. 6(a)], symmetric Gaussian pulses [Fig. 6(b)], two successive pairs of sech pulses but with the delay between them long enough [Fig. 7(a)]. The two unequal sech pulses in Fig. 6(a) have $\Omega_0=3.60$ and 3.58, respectively. The Gaussian pulses in Fig. 6(b) are defined as $\Omega_0^+(t)=\Omega_l^-(t)=4.9\exp[-(t-t_p)^2/\tau_0^2]$. As for in Fig. 7, the incident field can be approximately described by $\Omega_0^+(t)=\Omega_l^-(t)=3.59\{\text{sech}[(t-t_{p1})/\tau_0]+\text{sech}[(t-t_{p2})/\tau_0)]\}$. The time delay $\Delta t_p=t_{p2}-t_{p1}$ is set as 35 and 5 for Figs. 7(a) and 7(b),

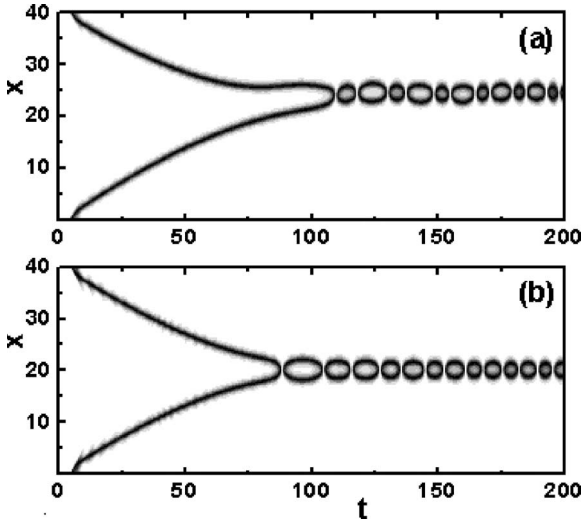

FIG. 6. Evolution of $n(x,t)$ under excitation by (a) two unequal sech pulses of $\Omega_0=3.6$ and 3.58, respectively, and (b) two equivalent Gaussian pulses of $\Omega_0=4.9$.

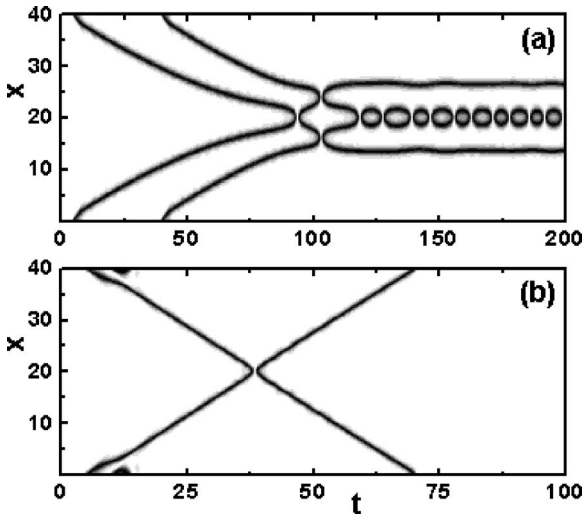

FIG. 7. Evolutions of $n(x,t)$ under excitation by four equal sech pulses of $\Omega_0=3.59$. The time delay between the first and second pair is (a) $\Delta t_p=t_{p2}-t_{p1}=35$, (b) $\Delta t_p=5$.

respectively. What occurs in Figs. 6(a), 6(b), and 7(a) is still that the excited GSs are stably trapped, which is even beyond our analytic prediction above and hence implies that the bound state is actually an attracting eigenstate of low energy for any unbalanced (keeping releasing linear waves) GSs of energies a little above it to evolve into. However, if shortening the time delay as in Fig. 7(b), the intense interaction between two adjacent GSs will exceed the slow decelerating effect of finite-length so that the former and latter GSs are directly pushed and repelled out, respectively, before they have time to evolve into that eigenstate. This property may be useful for releasing the stored optical energy in a nonlinear PC structure.

IV. CONCLUSION

In conclusion, the finite structural length can damage the vigorous balance of a GS by truncating it at the boundaries. For evolving into a new equilibrium, a truncated GS has to keep releasing linear radiations so that the speed of it is gradually decelerated. Such two counterpropagating GSs, if excited by the moderate incident field such that their initial speeds are low enough, can coalesce into a nonmoving bound state, which is a breatherlike low-energy state and attracts most unbalanced GSs of energy a little above it to evolve into. These results prove not to occur on an infinite domain and suggest the possible applications in optical energy storage and release, signal processing, quantum computing, etc. Finally, this effect is reasonably promising to generally exist in PC structures of other kinks of nonlinearity.

ACKNOWLEDGMENTS

This work was supported by the National Natural Science Foundation of China (Grant No. 10547109), Guangdong Province's Natural Science Foundation (Grant No. 04300170), and GDUT's Science Foundation (Grant No. 053028).

[1] *Nonlinear Photonic Crystals*, edited by R. E. Slusher and B. J. Eggleton (Springer-Verlag, Berlin, 2003).
[2] B. I. Mantsyzov and R. N. Kuz'min, Sov. Phys. JETP **64**, 37 (1986).
[3] G. Kurizki, A. E. Kozhekin, T. Opatrny, and B. A. Malomed, Prog. Opt. **42**, 93 (2001).
[4] J. P. Prineas, J. Y. Zhou, J. Kuhl, H. M. Gibbs, G. Khitrova, S. W. Koch, and A. Knorr, Appl. Phys. Lett. **81**, 4332 (2002).
[5] C. Conti, G. Assanto, and S. Trillo, J. Nonlinear Opt. Phys. Mater. **11**, 239 (2002).
[6] W. Chen and D. L. Mills, Phys. Rev. Lett. **58**, 160 (1987).
[7] A. B. Aceves and S. Wabnitz, Phys. Lett. A **141**, 37 (1989).
[8] M. J. Ablowitz and P. A. Clarkson, *Solitons, Nonlinear Evolution Equations and Inverse Scattering* (Cambridge University Press, Cambridge, 2000).
[9] N. G. R. Broderick, D. J. Richarson, and M. Ibsen, Opt. Lett. **25**, 536 (2000).
[10] J. W. Fleischer, T. Carmon, M. Segev, N. K. Efremidis, and D. N. Christodoulides, Phys. Rev. Lett. **90**, 023902 (2003).
[11] D. Mandelik, R. Morandotti, J. S. Aitchison, and Y. Silberberg, Phys. Rev. Lett. **92**, 093904 (2004).
[12] R. Fischer, Denis Träger, D. N. Neshev, A. A. Sukhorukov, W. Krolikowski, C. Denz, and Y. S. Kivshar, Phys. Rev. Lett. **96**, 023905 (2006).
[13] B. I. Mantsyzov and R. A. Sil'nikov, J. Opt. Soc. Am. B **19**, 2203 (2002).
[14] W. C. K. Mak, B. A. Malomed, and P. L. Chu, Phys. Rev. E **69**, 066610 (2004).
[15] B. I. Mantsyzov, I. V. Mel'nikov, and J. S. Aitchison, Phys. Rev. E **69**, 055602(R) (2004).
[16] D. W. McLaughlin and A. C. Scott, Phys. Rev. A **18**, 1652 (1978).
[17] M. Remoissent, *Waves Called Solitons* (Springer-Verlag, Berlin, 1999).
[18] M. Hübner, J. P. Prineas, C. Ell, P. Brick, E. S. Lee, G. Khitrova, H. M. Gibbs, and S. W. Koch, Phys. Rev. Lett. **83**, 2841 (1999).
[19] A. Kaso and S. John, Phys. Rev. E **74**, 046611 (2006)
[20] S. F. Mingaleev, A. E. Miroshnichenko, Y. S. Kivshar, and K. Busch, Phys. Rev. E **74**, 046603 (2006).
[21] Y. J. He and H. Z. Wang, Opt. Express **14**, 9832 (2006).
[22] J. Zhou, H. Shao, J. Zhao, X. Yu, and K. S. Wong, Opt. Lett. **30**, 1560 (2005).
[23] J. T. Li and J. Y. Zhou, Opt. Express **14**, 2811 (2006).